

Effects of the tilted and wavy current sheet on the solar modulation of galactic cosmic rays

Shoko Miyake and Shohei Yanagita

Faculty of Science, Ibaraki University, Mito 310-8512, Japan

Presenter: Shoko Miyake (miyakesk@cc.nao.ac.jp), jap-miyake-S-abs1-sh34-poster

Transport equation of the galactic cosmic ray (GCR) is numerically solved for $qA > 0$ and $qA < 0$ based on the stochastic differential equation (SDE) method. We have developed a fully time-dependent and three-dimensional code adapted for the wavy heliospheric current sheet (HCS). Results anticipated by the drift pattern are obtained for sample trajectories and distributions of arrival points at the heliospheric boundary for GCR protons. Our simulation reproduced a 22-year cycle of solar modulation which is qualitatively consistent with observations. Energy spectra of protons at 1 AU are calculated and compared with the observation by BESS.

1. Introduction

Transport of the galactic cosmic rays in the heliosphere is described by Parker's transport equation. The Parker's equation is equivalent to a coupled stochastic differential equation (SDE) [1, 2]. This SDE method allows us to get some information about solar modulation phenomena of galactic cosmic ray (GCR) not obtained by other numerical methods, such as distributions of arrival time, energy lost, and trajectory. We have developed a fully time-dependent and three-dimensional code based on the SDE method. We present some numerical results on solar modulation effects on GCR obtained by this new code.

2. The Model

The SDE equivalent to Parker's transport equation is written as [2]

$$\begin{aligned} d\mathbf{X} &= (\nabla \cdot \boldsymbol{\kappa} - \mathbf{V} - \mathbf{V}_d) dt + \sum_s \boldsymbol{\sigma}_s dW_s(t), \\ dP &= \frac{1}{3} P (\nabla \cdot \mathbf{V}) dt, \end{aligned} \quad (1)$$

where \mathbf{X} and P are the position and the momentum of the particle, \mathbf{V} is the solar wind velocity, \mathbf{V}_d is the gradient-curvature drift velocity, $\boldsymbol{\kappa}$ is the diffusion coefficient tensor, $\sum_s \sigma_s^\mu \sigma_s^\nu = 2\kappa^{\mu\nu}$, and dW_s is a Wiener process given by the Gaussian distribution. We adopted $V = 400$ km/s, $\kappa_{\parallel} = 1.5 \times 10^{21} \beta(p/(1\text{GeV}/c))(Be/B)$ cm²/s, $\kappa_{\perp} = 0.05\kappa_{\parallel}$, B is the magnetic field, and $Be = 5$ nT is B at the earth. We assume the structure of heliospheric magnetic field (HMF) as standard Parker spiral. We have used the "drift velocity field method" [3] for the calculation of drift in the heliospheric current sheet (HCS). In our simulation, particles start at 1 AU on the equatorial plane and run backward in time until they exit the heliospheric boundary, 80 AU.

We assume the structure of the HCS is as

$$\theta = \frac{\pi}{2} - \sin^{-1} \left[\left| \sin \left(\frac{\pi}{2} + \pi \frac{t - \frac{r-r_{\odot}}{V}}{11\text{years}} \right) \right| \sin \left(\phi - \phi_0 - \Omega_{\odot} t + \frac{(r - r_{\odot}) \Omega_{\odot}}{V} \right) \right], \quad (2)$$

where r , θ , ϕ are spherical polar coordinates relative to the solar rotation axis, ϕ_0 is a constant, r_{\odot} is the radius of the Sun, and Ω_{\odot} is the rotational angular velocity of the Sun. Similar expression for HCS had been adopted

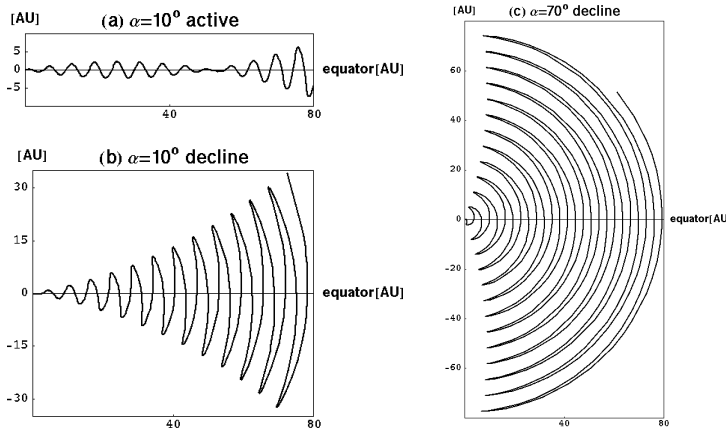


Figure 1. (a) A view of the HCS projected onto a meridional plane as a function of radial distance from the Sun. The tilt angle near the Sun is 10° , and the solar activity heading for the maximum; (b) Same as (a), but the solar activity heading for the minimum; (c) Same as (b), but the tilt angle near the Sun is 70° .

by Jokipii and Thomas [4], but with constant tilt angles contrary to our model. In this simple HCS model, the tilt angle changes continuously from 90° to 0° to 90° over a period of 11 year. The solar polarity of the HMF reverses when the tilt angle of HCS near the sun reaches 90° . Figure 1 shows views of HCS projected onto a meridional plane for three phases in the solar cycle. We have not taken into account in our model such phenomena as the global merged interaction regions, and the dynamically changing HCS with Fisk-like field [5].

3. Results

Figure 2 shows a sample trajectory for two protons which propagate from a point at 1 AU on the equatorial plane to 10 AU. The coordinate system of the figure is corotating with the sun. The drift pattern of the GCR depends on the polarity qA , where q is a charge sign of the sample particle and A is a constant characterizing HMF. For the positive polarity $qA > 0$, the particles drift from the polar region towards the HCS, and outward along the HCS. In contrast, for the negative polarity $qA < 0$, the direction of the drift is opposite to the case for $qA > 0$.

Figure 3 shows the heliolatitude-longitude distribution of simulated particles when they exit the heliospheric boundary, where the longitude is shown in the corotating coordinate system. The thick line indicates the HCS at 1 AU when the particles start off from a point (indicated by “star”) at 1 AU on the equatorial plane. Latitudes of the arrival points for $qA < 0$ distribute around the HCS as expected, because particles arrive at 1 AU along the HCS. The thickness of the distribution of latitude ($\pm 30^\circ$) reflects the structure of spatiotemporal variation of the HCS. The structure of the HCS seen by particles is different from particle to particle depending on the arrival time. On the contrary, the latitude for $qA > 0$ distribute around the polar region, either northern (a) or southern (b) depending on whether the observer is located at a point northern (a) the HCS or southern (b), respectively. This tendency is also as expected, because it is difficult for positive particles to penetrate through the HCS during the journey from the outer heliosphere. The mean arrival time of 1 GeV protons is 4.5 days and 80 days for $qA > 0$ and $qA < 0$, respectively. The short

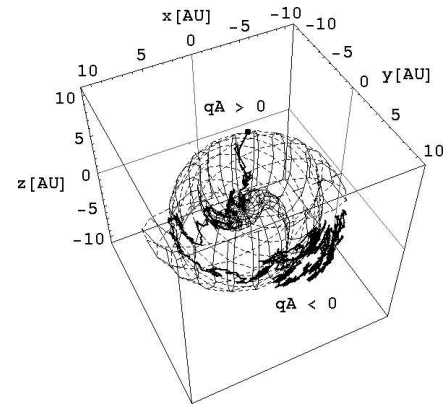


Figure 2. Sample trajectory for two protons. The tilt angle near the Sun is 40° , and the solar activity heading for the maximum. The energy at 1 AU on the equatorial plane is 1 GeV.

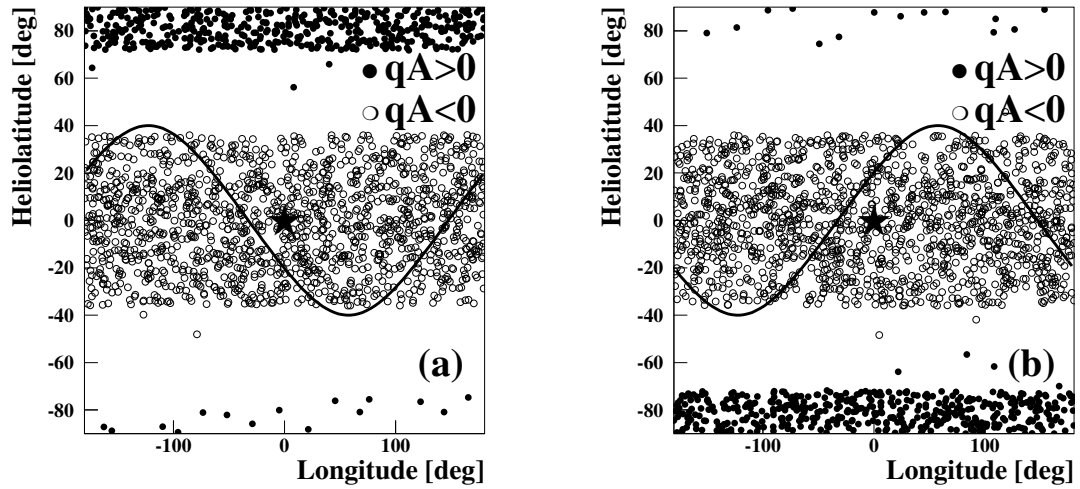


Figure 3. (a) Heliolatitude-longitude distribution by simulation for protons with energy 1 GeV at 1 AU when they exit the heliospheric boundary, 80 AU. The observer at 1 AU on the equatorial plane is located at a point northern the HCS; (b) Same as (a), but the observer is located at a point southern the HCS. The tilt angle near the sun is 40° , and the solar activity heading for the maximum.

time of only 4.5 days for $qA > 0$ suggests that particles are less modulated. This relatively little modulation effect is reflected in the fail to reproduce the observed spectrum for $qA > 0$ as we mention later.

Figure 4a shows simulated variation of the proton intensities over the 22-year modulation cycle. The solid line indicates the result for the model of the HCS by eq.2 ($\alpha(r, t)$ model). The dashed line shows the result for the HCS model ($\alpha(t)$ model) where the tilt angle varies with time but does not depend on radius from the sun. In our $\alpha(r, t)$ model, the variation of the HMF near the sun propagates with the solar wind velocity. It takes about 1 year for the signal of polarity change and change in the tilt angle reach the heliospheric boundary. In $\alpha(t)$ model, on the contrary, these changes reach instantaneously the boundary. This difference between the two models in signal propagation is reflected in a time lag of the proton intensity changes by $\alpha(r, t)$ model as seen in Figure 4a. Our model succeeded in reproducing a 22-year modulation cycle and in reproducing, though qualitatively, rather flat maximum for $qA > 0$ and a sharp maximum for $qA < 0$ [6].

Figure 4b shows proton energy spectra by our simulation (solid line) and the spectra observed by BESS experiment (open symbol). The open triangles refer to proton fluxes observed in 1998 [7] when the tilt angle near the sun is about 10° and the solar polarity is positive. The open squares refer to proton fluxes observed in 2000 [8] when the tilt angle near the sun is about 70° and the solar polarity is negative. The symbols for simulated energy spectra refer to the phases marked by the same symbol in Figure 4a. The view of the HCS corresponding to these phases are shown in Figure 1a and 1c. The local interstellar spectrum (LIS) of proton is assumed as $j_T \propto \beta(T + 0.5mc^2)^{-2.6}$, where T is kinetic energy and m is the mass of proton. The simulated energy spectra are normalized at 3.6 GeV to the observation in 2000 [8]. Our model spectrum for $qA < 0$ agrees quite well with BESS result, however our model fails to reproduce the observed spectrum for $qA > 0$. The failure of our model for $qA > 0$ may come from inadequacies of the heliospheric structure in our model. As we mentioned before, positive particles drift from polar region within short times modulated rather weakly. If we take into account the existence of the random transverse component of the HMF in the polar regions [9], we may be able to reproduce the observed spectrum because it is expected that the random transverse compo-

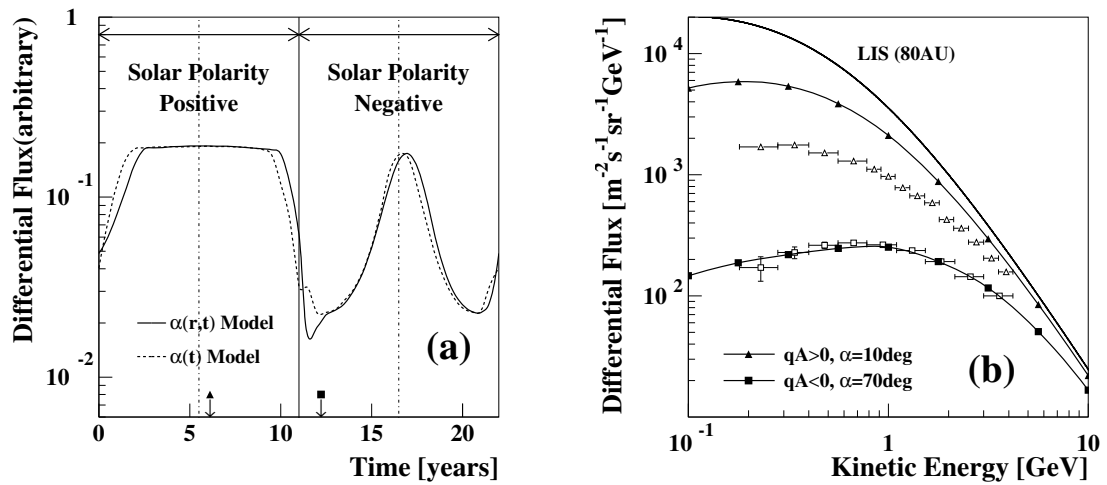


Figure 4. (a) Simulated variation of the 1 GeV proton intensities over the 22-year modulation cycle; (b) Simulated proton energy spectra and observed proton energy spectra in 1998 and 2000.

ment suppresses drifts in the polar regions. The actual variation of the HCS is much irregular in contrast to our model. We have to consider the actual dynamically changing HCS.

4. Conclusions

We have developed a time-dependent and three-dimensional code based on the SDE method. The sample trajectories and distributions of arrival points at the heliospheric boundary agree with the physical expectation. Our simulation reproduced a 22-year modulation cycle which is qualitatively consistent with observations. Our model spectrum for $qA < 0$ agrees with BESS result, however our model fails to reproduce the observed spectrum for $qA > 0$.

5. Acknowledgements

We would like to thank Prof. J. Kota and Prof. P. Evenson for their comments and suggestions on this work.

References

- [1] Yamada Y., S. Yanagita, and T. Yoshida, *Geophys. Res. Lett.*, 25, 2353-2356, 1998.
- [2] Zhang M., *Astrophys. J.*, 513, 409-420, 1999.
- [3] Burger R. A. and M. S. Potgieter, *Astrophys. J.*, 339, 501-511, 1989.
- [4] Jokipii J. R. and B. Thomas, *Astrophys. J.*, 243, 1115-1122, 1981.
- [5] Kota J. and J. R. Jokipii, 28th ICRC (Tsukuba), 3791-3794, 2003.
- [6] Webber W. R. and J. A. Lockwood, *J. Geophys. Res.*, 93, 8735-8740, 1988.
- [7] Maeno T. et al., *Astropart. Phys.*, 16, 121-128, 2001.
- [8] Asaoka Y. et al., *Phys. Rev. Lett.*, 88, 051101, 2002.
- [9] Jokipii J. R. and J. Kota, *Geophys. Res. Lett.*, 16, 1-4, 1989.